NeuroImage 174 (2018) 87–96

Contents lists available at ScienceDirect

NeuroImage

journal homepage: www.elsevier.com/locate/neuroimage

Cortical and subcortical responses to biological motion

Dorita H.F. Chang [a,*], Hiroshi Ban [b,c], Yuji Ikegaya [b,d], Ichiro Fujita [b,c], Nikolaus F. Troje [e]

[a] Department of Psychology, The University of Hong Kong, Hong Kong
[b] Center for Information and Neural Networks (CiNet), National Institute of Information and Communications Technology, Japan
[c] Graduate School of Frontier Biosciences, Osaka University, Japan
[d] Graduate School of Pharmaceutical Sciences, The University of Tokyo, Japan
[e] Department of Psychology, Queen's University, Canada

ARTICLE INFO

Keywords:
Visual perception
Biological motion
Life detector
fMRI

ABSTRACT

Using fMRI and multivariate analyses we sought to understand the neural representations of articulated body shape and local kinematics in biological motion. We show that in addition to a cortical network that includes areas identified previously for biological motion perception, including the posterior superior temporal sulcus, inferior frontal gyrus, and ventral body areas, the ventral lateral nucleus, a presumably motoric thalamic area is sensitive to both form and kinematic information in biological motion. Our findings suggest that biological motion perception is not achieved as an end-point of segregated cortical form and motion networks as often suggested, but instead involves earlier parts in the visual system including a subcortical network.

Introduction

The introduction of point-light motion displays (Johansson, 1973) has helped reveal the exceptional efficiency with which the human visual system can interpret animate (biological) motion devoid of other obvious contextual cues (e.g., the shape of the agent). Of course, form information is still readily available through the deformation of the motion pattern itself, and indeed observers use such global structure-from-motion information to interpret biological motion (Troje, 2002). It is clear now, however, that the global shape arising from deformation of the motion pattern is not the only cue available to the observer. Extensive behavioral data suggest that the visual system is also remarkably sensitive to local kinematic information, and particularly responds to the gravitational acceleration of the feet and the way they strike the ground (Beintema and Lappe, 2002; Troje and Westhoff, 2006; Chang and Troje, 2009). We refer to these two sources of information as "global" (structure from motion) and "local" (kinematics of individual dots) cues.

Neuroimaging, neurophysiology, and neurostimulation studies have identified a network of areas in the cortex that responds to biological motion. Relevant areas include ventral extrastriate regions such as the posterior superior temporal sulcus (pSTS), posterior inferotemporal sulcus (pITS), fusiform gyrus, extrastriate and fusiform body areas (EBA, FBA), but also portions of the frontal and parietal cortex (Bonda et al., 1996; Grossman and Blake, 2002; Peuskens et al., 2005; Saygin et al., 2004; Peelen et al., 2006; Saygin, 2007; Jastoff and Orban, 2009; Grosbas et al., 2012; Thompson and Baccus, 2012; van Kemenade et al., 2012). However, these studies have generally isolated the areas involved in the perception of biological motion by contrasting an intact walker with one that is spatially scrambled. This contrast addresses the effects of global structure on the neural responses well, but since the kinematic information conveyed by the individual local dots are the same between the two stimuli, it is not appropriate to search for the neural representations of local cues. Studies thus far that have tried to tease apart the separate contributions of shape and kinematics have promisingly shown some dissociation in terms of the cortical networks involved. Notably, the dorsal cortex seems to be critical for the perception of kinematics, and the ventral stream critical for the perception of shape (with information from the two streams proposed to be integrated in the occipito-temporal cortex) (Casile and Giese, 2005; Thompson et al., 2005; Jastoff and Orban, 2009; Vangeneugden et al., 2014; Gilaie-Dotan et al., 2015). While the majority of these studies have reduced biological motion into point-light representations, these same regions are implicated in more naturalistic contexts. For example, videos and static images of bodies similarly elicit responses in ventral body areas EBA and FBA (O'toole et al., 2014).

There is reason to believe that surveys of the brain regions relevant to biological motion perception would benefit from moving beyond the cortex, considering the roles of subcortical loci. The neural substrates underlying the perception of local kinematics, in particular, has garnered

* Corresponding author. Department of Psychology, The University of Hong Kong, 6.07, The Jockey Club Tower, Centennial Campus, Hong Kong.
E-mail address: changd@hku.hk (D.H.F. Chang).

https://doi.org/10.1016/j.neuroimage.2018.03.013
Received 13 October 2017; Received in revised form 28 February 2018; Accepted 5 March 2018
Available online 8 March 2018
1053-8119/

much intrigue as it is posited that the relevant mechanisms are phylogenetically more primitive, and hence likely to involve older parts of the visual system (Troje and Westhoff, 2006; Johnson, 2006). In light of a growing body of developmental data showing that sensitivity to biological motion is present early in development (Fox and McDaniel, 1982; Bertenthal, 1996; Hirai and Hiraki, 2005; Méary et al., 2007; Reid et al., 2008), it would not be surprising if biological motion perception is governed in part by deeper structures such as the brainstem or thalamus. This line of thought is also strengthened by work in non-human species - newly hatched chicks - for orienting towards biological motion (Vallortigara et al., 2005; Vallortigara and Regolin, 2006). These findings in chicks, which have very different brain organization as compared to primates, though they do have circuits elsewhere with functions homologous to those governed by the mammalian six-layer cortex (Wang et al., 2010), should challenge our traditional understanding that high-order "biological motion" perception in humans is solely reliant on the cortex.

While the thalamus has been long-considered a sensory relay center, an increasing body of literature is indicating a regulatory role for this region, contributing to wide-ranging aspects of cognition. For example, it has been shown that fMRI responses in the human lateral geniculate nucleus (LGN) can be modulated by actively directing subjects to attend to or ignore a stimulus (O'Connor et al., 2002). Attentional modulations of single-unit responses in the LGN have also been shown in the macaque (McAlonan et al., 2008). Moreover, lesions in the thalamus, and in particular of the pulvinar and mediodorsal nucleus, can result in attention and memory impairments (e.g., Baxter, 2013; Jankowski et al., 2013). Considered together, these findings challenge traditional notions that attentional modulations have sole cortical origins. Beyond attentional processes, thalamic nuclei have been implicated in other high-order functions including learning (Bradfield et al., 2013; Habib et al., 2013), language (Klostermann, 2013), and movement control (e.g., Prevosto and Sommer, 2013) – extending to anticipations of perceptual consequences of ocular movements (Ostendorf et al., 2013). Hence, it would not be surprising if the thalamus, and potentially other subcortical centers may also be implicated in biological motion perception.

To our knowledge, only one study to date has implicated a non-cortical area (the cerebellum) in the processing of biological motion (Sokolov et al., 2012). These findings are particularly interesting at it has become increasingly clear that the cerebellum should no longer be considered a solely motor structure. For example, the cerebellum has been shown to be involved in language processing (e.g., Xiang et al., 2003), visuospatial reasoning (e.g., Bonda et al., 1995; Creem-Regehr et al., 2007), and executive functions (e.g., Tomasi et al., 2007). Whether additional subcortical components of the motor loop may be involved in a broader range of functions, including, of more immediate relevance, the perception of biological motion, is unclear.

Here, using whole-brain, high-resolution, multiband fMRI, along with a multivariate approach (multivoxel pattern analysis, MVPA), we aimed to achieve a survey of the cortical and subcortical areas for the perception of global structure-from-motion and local kinematic information in biological motion that may have been overlooked in traditional univariate approaches. We focus on global and local cues containing information about the intended walking direction of a stationary point-light walker. The facing-direction task has been used widely to show the importance of both form-related processes (Beintema and Lappe, 2002; Miller and Saygin, 2013) and kinematics-related processes (Troje and Westhoff, 2006; Hirai et al., 2011) in biological motion perception. We introduced three main types of manipulations in order to isolate stimuli that contained solely global form from motion information, solely kinematics, or neither global form nor natural kinematics information. To isolate representations of global structure-from-motion we generated novel walkers that carried the structure of an intact walker but no informative local cues as to walking direction ("global only" walkers). These stimuli were generated by replacing each local trajectory with the average of its original trajectory and its left/right mirror-flipped variants. While the overall spatial arrangement of the dots was preserved, this manipulation rendered individual local motions that were symmetric along the anterior-posterior axis, and critically carried no horizontal asymmetry. In order to create a stimulus that isolates local cues to facing direction, stimuli were deprived of structural cues to direction by taking the veridical walker (Troje, 2002) and randomly reallocating the positions of the individual dots along the horizontal dimension. We call this stimulus the "local natural" walker. We then took this latter stimulus and modified it further in order to also deprive it from the acceleration patterns that we had earlier shown to be the critical feature of the "life detector" (Chang and Troje, 2009). This last type was achieved by both scrambling the horizontal positions of the individual dots thereby destroying global structure, and manipulating kinematics such that the individual dots traveled along the original traces at constant speed (Chang and Troje, 2009). We call this stimulus the "local modified" walker (see Methods for further details on the stimulus manipulations). The three types of walkers were presented both upright and upside-down. We included an 'inversion' manipulation to help validate any dissociations between structure-related and kinematics-related regions, in light of behavioral literature that have suggested very different sources underlie inversion-related perceptual impairments for the two types of stimuli. The source of the first inversion effect appears to be similar to that observed in the face literature (Freire et al., 2000), relating to the inversion of the familiar (body) structure. The inversion effect observed with kinematics-only stimuli, however, appears to relate to the orientation of velocity gradients within the individual dot-motions, and specifically those of the feet, but is also curiously modulated by visual field position (Chang and Troje, 2009; Hirai et al., 2011). Inclusion of the upside-down variants, thus probe for differential modulations of the relevant regions with inversion and may thereby help verify any dissociation between structure-related and kinematics-related regions.

Methods

Participants

Nineteen observers (mean age of 26.4 years, 13 males) participated in this study. All had normal or corrected-to-normal vision, and provided written informed consent in line with ethical review and approval of the work by the ethics committee of the National Institute of Information and Communications Technology (NICT), Japan.

Stimuli

Stimuli were point-light biological motion sequences based on motion capture data of an average walker computed from 50 men and 50 women, that can be represented as a simple fourier series characterizing the position of each dot motion in three dimensions (Troje, 2002). Each walker in this particular experiment was represented by a set of 11 dots shown in sagittal view (facing either rightward or leftward) with a gait frequency of 0.93 Hz. Overall translation was subtracted. Dots were white (153.7 cd/m^2) on a black background (0.92 cd/m^2).

The average walker in its original form contains both full structure from motion information (through the presence of the familiar body shape) and kinematic information (as carried by horizontal and vertical asymmetries, such as acceleration). In order to tease apart the contributions of these differing types of information, we did not present the walker in this original form, but rather derived six variations of the stimulus, manipulating the presence or absence of structural organization (intact or absent), the kinematic information contained in the individual local trajectories (veridical kinematics, mirror-symmetric motion, or perturbed-constant speed), and orientation (upright or inverted). As these manipulations cannot be neatly characterized in terms of a factorial-type design, we provide schematic samples of the stimuli (Fig. 1a), as well as summarize the information contained in the stimulus in accordance with our stimulus labels, both in terms of global structure

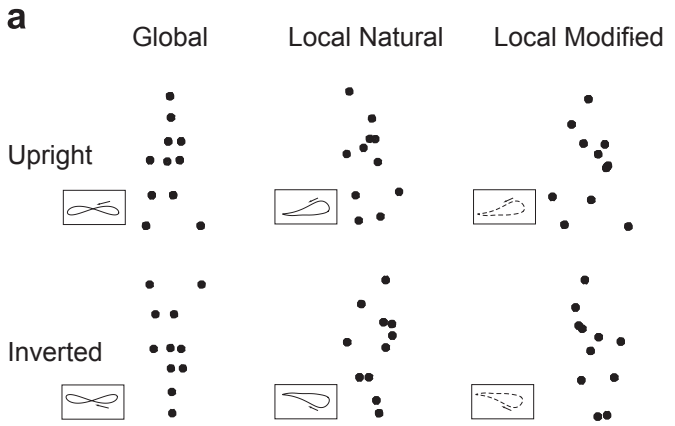

b

Stimulus label	Information Contained	
	Global Structure	Local Trajectories
Global	Intact	Symmetric
Local Natural	Scrambled	Veridical
Local Modified	Scrambled	Constant

Fig. 1. Schematic representations of the three main types of stimuli presented in this experiment, at the two orientations (Fig. 1a). In the global stimulus, the structural organization of the walker was held intact, but local trajectories were rendered left-right mirror symmetric. In the local natural stimulus, the structural organization was destroyed by horizontal shuffling, but the local kinematics were veridical. Finally in the local modified stimulus, both the structural organization was destroyed through horizontal shuffling, and local kinematics were perturbed by forcing the motion along the fixed trace at constant speed. The stimulus labels and the corresponding global and local information contained in them are summarized in Fig. 1b.

and local kinematics (Fig. 1b**).**

Samples of the stimuli can also be viewed at http://changlab.hk/demo-bm. All demonstrations in the multimedia are right-facing.

Global only walker

Our "global only" walker was designed to convey structure-from-motion information only, by rendering individual local trajectories (left-right) mirror-symmetric. This was achieved by first preserving the spatial layout of the dot trajectories (i.e., the mean position of each dot is retained in its original vertical and horizontal location). Critically, we then took each individual point-light motion and replaced its horizontal component by the average of the original trajectory and its left/right mirror-flipped variants. The resulting motion is perfectly symmetric about the horizontal axis. This is conveyed in Fig. 1a (global walker and its inset) where we have provided the trace of one dot – that of the foot trajectory of our global walker. This left/right symmetric motion can be contrasted with that of the natural walker (Fig. 1a, local natural walker, inset), which, if in motion, retains strong horizontal asymmetric cues in one direction (i.e., left, in Fig. 1a). Consequently, in the global walker, kinematic-based direction cues are now uninformative. If asked to resolve the facing direction of such a stimulus, the observer can only rely on the deformation of the overall structure (from motion). Certainly, as this manipulation indeed provides distortions to the shape of the local trajectories themselves, one could argue that the overall structural deformation of the walker is also not entirely identical to that which would be carried by a veridical walker (although casual inspection of our interactive demo reveals that any distortions to global shape appear rather minimal).

Local natural walker

Our "local natural" walker was designed to carry natural kinematic information, but no global structure information. This walker was achieved by starting with the original (average) walker and randomly shuffling the horizontal spatial positions of the dots. There were no manipulations to the local kinematics. As such, if asked to resolve the facing direction of this particular stimulus, the observer can rely on local kinematics, but not global structural deformations.

Local modified walker

Finally, a "local modified" walker was designed to carry neither structure-from-motion information nor valid kinematic information. This walker was achieved by starting with the original (average) walker and, as for the "local natural" walker, randomly shuffling the horizontal spatial positions of the dots; however, we additionally perturbed local motion by forcing each individual dot to move with constant speed along its original trajectory. That speed was equal to the average speed of the corresponding dot-motion in the original walker (Chang and Troje, 2009). This was achieved by interpolating each individual dot trajectory and computing linear arclength. Critically, this manipulation disrupts the natural velocity profile of the foot motion and in particular eliminates the vertical asymmetries caused by gravitational acceleration. This walker then contains neither global form information nor the critical local invariants.

The three types of stimuli (global only, local natural, and local modified) were shown upright or inverted, rendering a total of six main stimulus variations. Importantly, an inverted "local natural" and "local modified" walker was generated by mirror-flipping each dot about its horizontal axis only. This retains the vertical order of the dots (i.e., feet dots were retained at the bottom of the display). An inverted "global only" walker carried a complete inversion of the shape and the local trajectories (which were themselves altered, as described above). For all stimuli, the starting phase (temporal position of the gait cycle) was randomly selected on each trial. For the two "local" stimuli, horizontal spatial shuffling was randomized on each trial.

Stimuli were presented on a PC (HP Z230SF). Graphics rendering was implemented by a nVidia Quadro K600 graphics card set to display 1024×768 pixels at 60 Hz. Stimuli were front-projected to a screen placed 90 cm from back of the bore using a LCD projector (Cannon WUX4000) and viewed through a 45 deg tilted mirror mounted in front of the observer. Stimuli subtended visual angles of 2.9×6.4 deg.

Biological motion task

On each trial, participants were presented with a single point-light walker (500 ms) and asked to judge whether the walker appeared to be facing rightwards or leftwards by responding with one of two buttons on the response box. Each trial was allotted a fixed inter-stimulus interval of 1500 ms, before it timed out and the subsequent trial presented. A central fixation cross (0.5×0.5 deg in size) was presented for the full duration of each trial. Observers were asked to respond after stimulus offset.

fMRI acquisition

Imaging data for the participants were acquired at the NICT CiNet imaging facility (Suita, Osaka, Japan), using a 3-T Siemens Trio MR scanner with a 32-channel, phase-array (whole) head coil for both localizer and experimental runs. Blood oxygen level–dependent signals were measured with an echo-planar sequence (Voxel size = 1.5 mm^3, TR = 2000 ms, Flip angle = 70 deg, 78 slices with multiband (factor = 3); 205 vol where the first 5 were discarded to eliminate the effects of start-up transients). The Multi-Band EPI sequence was provided by the University of Minnesota (under a C2P contract). For each participant, we additionally acquired a high-resolution (1 mm^3) anatomical scan.

ROI definition

Regions-of-interest (ROIs) V1, V2, V3, V4, V3A, and V3B/KO were defined for each participant using standard phase-encoded retinotopic

mapping procedures, mapping polar angle with a slowly rotating (clockwise or counterclockwise), checkerboard wedge stimulus (Sereno et al., 1995). We were able to identify V3B/KO (kinetic occipital) using this same phase-encoded map (Wandell et al., 2005; Ban et al., 2012), generally falling anterior to V3A, inferior to V7 (Dupont, 1997) and posterior to the human motion complex (hMT+/V5). We subsequently identified hMT+/V5 in each participant using a separate functional localizer (single-run), defining it as the region that responded significantly higher ($p < 0.01$) to moving dots that traveled toward and away from fixation than to static dot fields (Huk et al., 2002). We included four additional extrastriate regions that have been previously implicated for biological motion perception. Each was defined as a spherical ROI (5 mm rad.) centered on Talairach coordinates of: [±36, 10, 28] for the inferior frontal gyrus (IFG) (Saygin et al., 2004; Saygin, 2007), [±57, ±45, 10] for the posterior superior temporal sulcus (pSTS) (Sunaert et al., 1999), [left −45, −74, 1; right 48, -70, 1] for the extrastriate body area (EBA) (Peelen et al., 2006; Jastoff and Orban, 2009), as well as [left 36, -39, −19; right 41, -45, −19] for the fusiform body area (FBA) (Peelen et al., 2006; Jastoff and Orban, 2009). We note that due to the proximity of the human motion complex hMT+ with EBA, overlapping voxels of the two regions, if any, were removed from both ROIs in each subject. Finally, VLN was identified post-hoc anatomically as an ROI defined by the Talairach atlas (Talairach et al., 1988). As this thalamic sub-area has no distinctive physical characteristic that can allow it to be identified in individual subjects through visual inspection, and has no known reliable functional localizers, we opted to use this common ROI across all subjects. The VLN, identified in this manner had coordinates of [-15, −10, 9.9] and a volume of 573 mm^3 for the left hemisphere, and coordinates of [13, −10, 10] along with a volume of 572 mm^3 for the right hemisphere.

Design and procedures

fMRI runs were arranged in a block-design with each block lasting 16 s. One particular scan run included five main block types comprising four stimulus condition blocks (e.g., global) and a fixation block. Each stimulus condition block was repeated 3 times within a particular run, and were interleaved by fixation blocks. Block order was randomized. Individual condition blocks consisted of 8 trials of a particular stimulus condition where the number of left and right-facing walkers were balanced within the block. Therefore, one particular run included 24 trials of a particular condition, and a total of 96 experimental trials. Due to the large number of conditions, stimulus conditions were scanned across two run types. Conditions global (upright), global (inverted), local natural (upright), and local natural (inverted) were acquired in Run type 1. Conditions local modified (upright), local modified (inverted) were acquired simultaneously with local natural (upright), and local natural (inverted) in Run type 2. Both run types were scanned in the same day (total session duration of 1.5 h), with the order of the run types within a session counterbalanced. These experimental scans were acquired on a separate day from the localizer scans. Participants completed a minimum of 8 total runs (4 scan runs per run type) yielding 96 trials per stimulus type (i.e., 12 “blocks” of trials). Each run lasted 6.8 min.

fMRI data analysis

fMRI data were analyzed with BrainVoyager QX (BrainInnovation B.V.). For each participant, we transformed anatomical data into Talairach space. Functional data were preprocessed using three dimensional motion correction, slice time correction, linear trend removal and high-pass filtering (3 cycles/run).

Data were subsequently analyzed both in terms of their univariate activity (GLM), and multivariate patterns (multivoxel pattern analysis, MVPA). GLM analyses included regressors for each experimental condition, and six motion regressors (three translation parameters; in millimeters) and three rotation parameters (pitch, roll, yaw; in degrees) defined as square-wave regressors for each stimulus presentation block convolved with a gamma function to approximate the idealized haemodynamic response. The time course signal of each voxel was then modelled as a linear combination of the different regressors (least-squares fits) and the regressor coefficients were used for contrasts of the different experimental conditions. Contrasts were performed after combining the two different run types, and included: For each stimulus orientation (upright and inverted), we contrasted global vs local natural (to elucidate form based representations) stimuli, and local natural vs local modified stimuli (to elucidate kinematic based representations). We additionally contrasted responses of the two orientations within each stimulus type (e.g., global upright vs global inverted). Whole-brain, group-level responses were analyzed using GLM random-effects analyses.

For the multivariate classifications, we chose to use a linear SVM classifier (libSVM) (Chang and Lin, 2011) together with a multivariate feature selection algorithm, Recursive Feature Elimination (RFE) to estimate spatial patterns (De Martino et al., 2008). The RFE eliminated the necessity of selecting a somewhat arbitrary fixed number of voxels per ROI, and instead offered estimates based on voxel subsets with the best performance within each ROI. Briefly, for this analysis, all voxels and their time courses were first converted to Z scores and shifted in time (4 s) to account for the hemodynamic response. This shift corresponds to the typical peak of the BOLD response function (Serences, 2004). We then took 80% of the *training data set* to compute SVM weights. Note that the sampling of data for training was done while retaining blocks in their entirety (i.e., no blocks were partitioned). The selection of the data set (and computation of SVM weights) were repeated 20 times within a particular RFE step (i.e., each voxel had 20 sampled weights, which were subsequently averaged). Following each step, we then ordered voxels based on their (step-averaged) weight from the highest to the lowest. Using these weights, we omitted the 5 most uninformative voxels, and used the rest to decode the *test patterns*. This yielded an accuracy at the current voxel count/pattern. This process was repeated until voxel count fell below 50. For each ROI, based on the maximum mean accuracy (across all cross-validations) across all RFE steps, we retrieved the final voxel pattern with which to compare the accuracies of the different cross validations. Mean prediction accuracies were tested against chance level (0.54), which was determined via permutation tests for the data (i.e., by running 1000 SVMs with shuffled labels).

As noted earlier, due to the large number of conditions in each experiment, conditions were scanned across two different run types. This resulted in an unbalanced training data set that was corrected via the Synthetic Minority Over-sampling Technique (SMOTE) algorithm (Chawla et al., 2002).

Behavioral data analysis

Behavioral performances were quantified in terms of the proportion of correct discrimination responses. As response input on each trial was not permitted until after stimulus offset, reaction time data were not considered informative and not analyzed. Discrimination accuracies were analyzed with a repeated-measures analysis of variance (ANOVA) comparing orientation (upright/inverted) and walker type (global only, local natural, local modified). Data were verified to satisfy parametric assumptions, and any variance (sphericity) violations were addressed with Greenhouse-Geisser corrections. Follow-up post-hoc comparisons were conducted by means of Bonferroni-corrected t tests (two-tailed).

Results

Behavioral discriminations

Behavioral performance, quantified in terms of proportion of corrected responses, were computed for each walker condition at the two orientations and are presented in Fig. 2. These accuracies were entered in a 2 (orientation) x 3 (condition) repeated-measures ANOVA that indicated performance was higher when the walkers were displayed

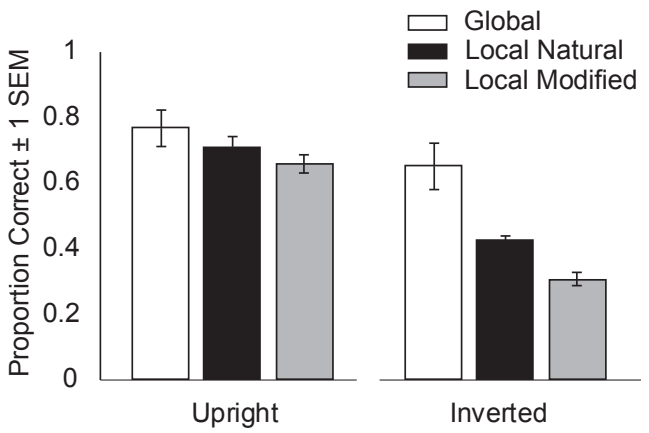

Fig. 2. Behavioral discrimination accuracies for direction judgements. Overall performance was significantly better for the upright rather than inverted stimuli. Performance was best for the global (empty bars), than the two local stimuli (black- and grey-filled bars). Additionally, inverting stimulus orientation resulted in a significant performance decline for the local natural and local modified stimuli, but not the global walkers. Error bars represent ±1 SEM (N = 19).

upright rather than inverted (main effect of orientation, $F(1,18) = 103.8$, $p < .001$, $\eta^2 = .85$), and varied according to walker condition (main effect of condition, $F(2, 36) = 16.7$, $p < .001$, $\eta^2 = .48$). Follow-up Bonferonni-adjusted t tests indicated that performance was highest for the global condition than for the two local conditions ($t(18) = 3.04$, $p = .021$ for global versus local natural; $t(18) = 4.65$, $p = .001$ for global versus local modified). Performance for the local natural stimuli was also generally better than that for the local modified stimuli, $t(18) = 7.08$, $p < .001$. Performance changes with stimulus inversion, however, depended on the type of stimulus (stimulus by orientation interaction, $F(2, 36) = 8.23$, $p = .001$, $\eta^2 = .43$). Specifically, inversion resulted in a significant performance decrease for the local natural stimuli, $t(18) = 11.8$, $p < .001$, local modified stimuli, $t(18) = 10.5$, $p < .001$, but only marginally for the global walkers, $t(18) = 1.9$, $p = .07$.

fMRI

Cortex

We first present the univariate (GLM) responses to our stimuli, in terms of the beta weights (% signal change) across our group of ROIs in Fig. 3, separately for the upright stimuli (upper panel) and inverted stimuli (bottom panel). We also present a sample map from the group-level whole-brain random-effects GLM analysis, contrasting the local natural versus local modified stimulus (Fig. 4). An initial comparison of the ROI-based analyses and the whole-brain maps indicated that our choice of ROIs adequately represented much of the univariate responses to our stimuli, with strong responses in retinotopic (V1-V4), and extrastriate areas – notably along the posterior STS, IFG, and EBA.

An examination of the beta weights revealed that signals were generally strongest for hMT+ as compared to all other cortical ROIs, and highest for the local natural stimuli as compared to the other two walker types. These observations were confirmed by a 3 (condition) x 2 (orientation) x 12 (ROI) repeated-measures ANOVA that indicated a significant main effect of condition, $F(2, 36) = 6.4$, $p = .004$, $\eta^2 = .26$, and a significant main effect of ROI, $F(3.9, 71.6) = 7.8$, $p < .001$, $\eta^2 = .30$. Post-hoc Bonferonni-corrected t-tests confirmed that weights for the global stimuli were significantly lower than those of the local natural stimuli, $t(18) = -2.9$, $p = .009$, but not different from those of the local modified stimuli, $t(18) = .14$, $p = .88$. Additional follow-up comparisons for the main effect of ROI confirmed that overall, the signals were higher for hMT + than for all

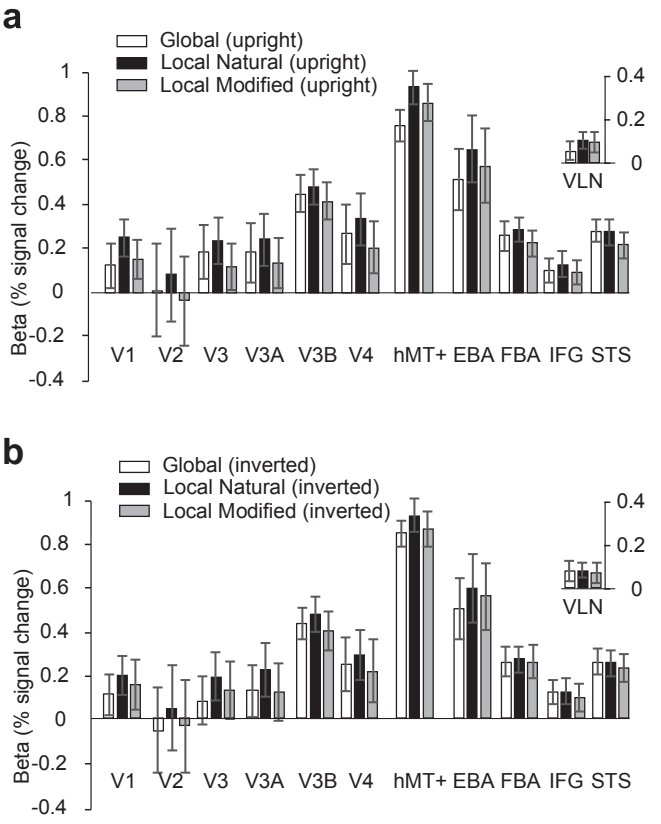

Fig. 3. GLM beta weights (% signal change) for the three main types of walkers at the upright (a) and inverted (b) presentations. Overall, the univariate signals were highest for the local natural stimuli. Note that in all multivariate analyses, the univariate differences across conditions were removed.

other ROIs (all comparisons involving hMT+, ps < .03). Additionally, while signals for V3b and EBA were significantly lower than that of hMT+, they were higher than those of all remaining ROIs (ps < .03). The ANOVA also indicated a significant interaction between condition and ROI, $F(6.1, 110.4) = 3.2$, $p = .005$, $\eta^2 = .15$. We interpreted this interaction with follow-up Bonferonni-corrected one-way ANOVAs for each condition (walker) type. The analyses indicated that the pattern of responses across ROIs was slightly different for the local modified stimulus as compared to the global and local natural stimuli. In particular for the global and local natural stimuli, responses for V3b were different from those of hMT+, IFG, and VLN (all *ps* < .03) while for the local modified stimulus, V3b responses did not differ from those of IFG ($p > .9$).

MVPA classification accuracies for discriminating stimuli containing global shape-from-motion versus local kinematic information (global vs. local natural walker) are presented in Fig. 5a (open bars). The classification accuracies of all ROIs were tested with t-tests against a baseline of 0.54 (see Methods), using False Discovery Rate (FDR) corrected thresholds that hold FDR < .05. Accuracies were well above-baseline in early retinotopic (V1-V4) and higher order areas including hMT+, EBA, FBA, IFG, and pSTS. These same areas had above-baseline classification accuracies for discriminating between intact and perturbed local kinematics (local natural vs. local modified) (Fig. 5a, filled bars, accuracies above shuffled-baseline, FDR <0.05). Differences among the walker types emerge when considering discriminations between upright and inverted stimuli. For global shape, a number of regions including early visual cortex, and hMT + can well discriminate between the two orientations; however, classification accuracies for discriminating upright versus inverted stimuli for local natural and local modified stimuli, did not differ from baseline for all ROIs (Fig. 5b).

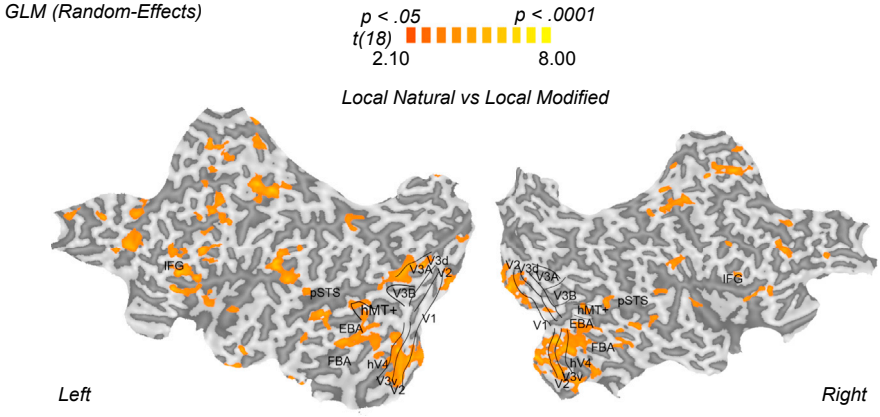

Fig. 4. Sample map from the whole-brain group-level GLM analyses (random effects). We present the results from contrasting responses to the local natural versus local modified stimulus. Responses are superimposed onto representative flat maps of left and right hemispheres of one participant, with retinotopic regions delineated. Sulci are coded in darker grey than the gyri.

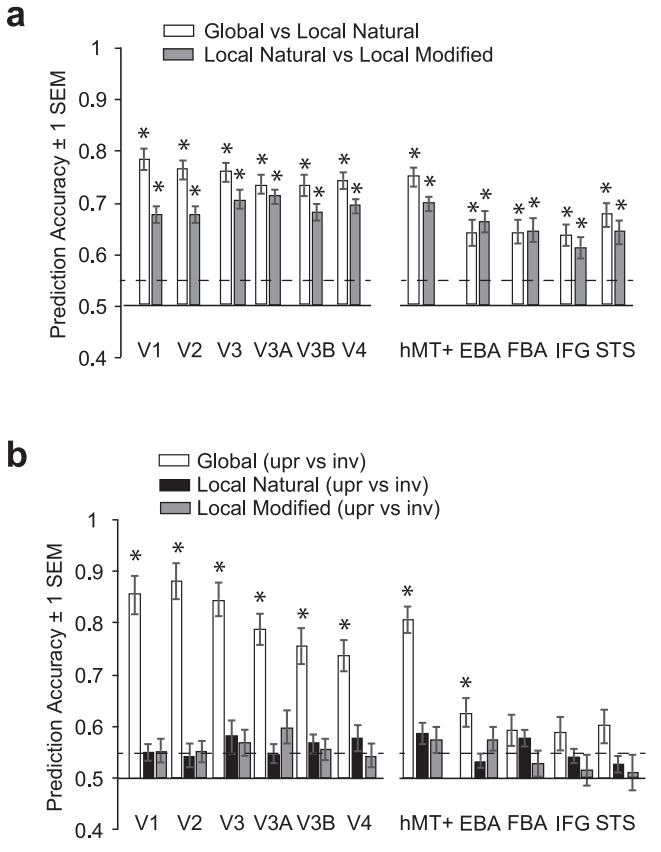

Fig. 5. MVPA classification accuracies are above-baseline for (a), discriminating global structure-from-motion from local (natural) kinematics, and between natural versus modified local kinematics; (b) discriminating between upright and inverted global and local cues. The dashed line indicates the shuffled baseline (0.54) against which accuracies were tested. Above-baseline accuracies (FDR < 0.05), are indicated by asterisks. Error bars represent ±1 SEM (N = 19).

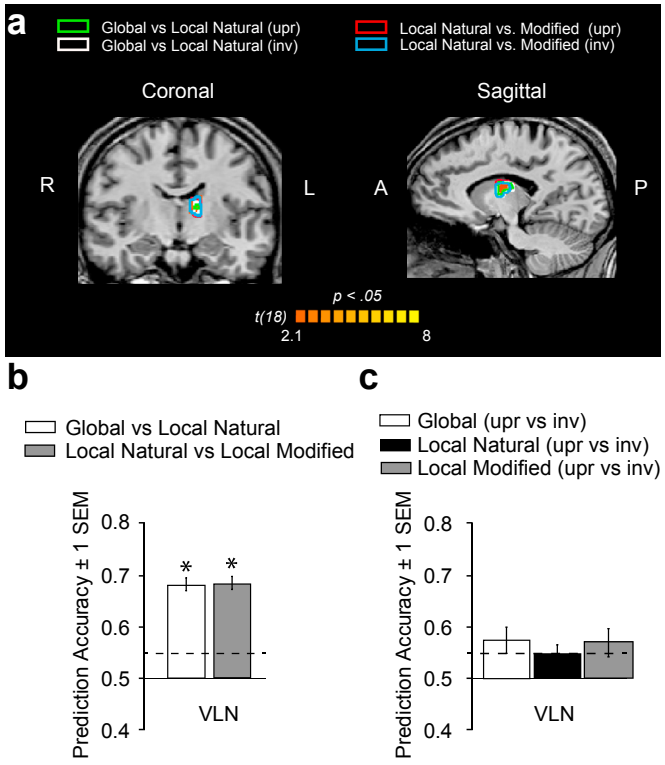

Fig. 6. (a) GLM contrasts for global shape-from-motion vs local (natural) kinematics (upright: green outline; inverted: white outline), and local natural vs modified kinematics (upright: red outline; inverted: blue outline) yielded significant, overlapping clusters in left ventral lateral nucleus (VLN). (b,c) Classification accuracies from ROI-based SVM analysis on bilateral VLN identified across subjects. The dashed line indicates the shuffled baseline (0.54) against which accuracies were tested. Above-baseline accuracies (FDR < 0.05), are indicated by asterisks. Error bars represent ±1 SEM (N = 19).

fMRI

Ventral lateral nucleus (VLN)

An examination of the univariate (General Linear Model) responses in subcortical regions revealed a thalamic area, specifically the left ventral lateral nucleus (VLN) that was involved in all contrasts including both those comparing global shape and local kinematics, as well as comparing local kinematics intact and perturbed (Fig. 6a, overlaid outlines).

We subsequently ran ROI-based SVM classifications on the VLN, as identified for all subjects by probabilistic and Talairach atlases. Accuracies for discriminating between global structure and local kinematics, as well as between the two local stimuli were well above chance in the VLN (Fig. 6b**; see also** Supplementary Figs. S2 and S3 **for lateralized analyses indicating above-chance classification performance independently in both the right and left VLN**). This was confirmed by t-tests of the accuracies against the baseline of 0.54, corrected (thresholded) to hold FDR < .05 ($t(18) = 5.5$, $p < .001$ for global versus local natural; $t(18) = 6.9$, $p < .001$ for local natural versus local modified). It is interesting to note that the VLN is however insensitive to both orientation of global structure and local kinematics (Fig. 6c). This is in contrast to above chance-level accuracies for discriminating global structure from local kinematics observed in the cortex (Fig. 5b), but congruent with the poor discrimination accuracies in these same regions when contrasting

orientations of natural and modified kinematics.

Finally, we conducted further analyses examining classification performance separately for the left and right hemispheres across all cortical ROIs (and VLN). The results are presented in Supplementary Fig. S1 (left hemisphere) and Fig. S2 (right hemisphere). Classification accuracies were entered in a 2 (hemisphere) x 5 (classification) x 12 (ROI) repeated-measures ANOVA. The analysis revealed that performance was comparable between both hemispheres (no significant main effect of hemisphere, $F(1, 18) = .06$, $p = 0.80$; no significant interactions involving hemisphere).

Discussion

We used carefully designed stimuli that contained solely biological form (global only stimulus), solely biological kinematics (local natural stimulus), and neither form nor kinematic information (local modified stimulus) in order to survey the neural representations of biological motion in cortex and subcortical structures.

While results from the analyses of univariate responses revealed rather homogenous activity across conditions, consideration of multivariate patterns is more revealing. We found a striking capacity of cortical regions for discriminating stimuli containing global and local information. Global shape-from-motion and local kinematic information (global vs. local natural walker) can be distinguished in early retinotopic areas (V1-V4) and higher order areas including EBA, FBA, IFG and STS – areas implicated previously for biological motion perception. This same broad network can also discriminate between intact and perturbed local kinematics (local natural vs. local modified). The ability of the STS to discriminate both global and local cues is surprising, given the relatively weak univariate signals this region produces when presented with walking (rather than action-type) stimuli (see also Jastoff and Orban, 2009); still, strong prediction accuracies can be observed in this region (and across cortex).

Intriguingly, results from both our GLM and MVPA analyses indicated a cluster outside of cortex - in a region identified as the ventral lateral nucleus that was responsive to our stimuli. The VLN holds extensive projections to the motor and premotor cortex (Kievit and Kuypers, 1975; Shinoda et al., 1993) and receives considerable afferents from the cerebellum (dentate nucleus) and the globus pallidus (Carpenter and Strominger, 1967). As such, the VLN is classically thought to act as a major relay for motor planning and coordination (e.g., Daskalakis et al., 2004), and is hence usually designated as part of the *motor thalamus*. Projection targets from the VLN, however, are not limited to motor cortex, but also include frontal and parietal associative cortex (e.g., Kievit and Kuypers, 1977; Wiesendanger and Wiesendanger, 1985a,b; Morel et al., 2005; Prevosto et al., 2009). In fact, the many cortical areas (i.e., prefrontal, frontal, parietal cortices) that provide input to the cerebellum also conversely receive cerebello-thalamo-cortical projections (Ramnani, 2012). Hence, the motor division of the thalamus, including in particular the VLN certainly has the circuitry to support higher-order functions. Indeed, several studies have suggested that the regions of the motor thalamus that receive cerebellar input (such as the ventral lateral complex) in fact contribute to executive control functions of the frontal lobe (Ide and Chiang-shan, 2011; van der Salm et al., 2013). For example, the cerebello-thalamo-cortico circuit has been shown to be involved behavioral adjustments in response to error detection (Ide and Chiang-shan, 2011). There is also an emerging line of evidence that suggests cortical regions with extensive cerebellar-thalamic input is involved in cognitive and motor aspects of language and memory (Johnson and Ojemann, 2000).

Nonetheless, our finding of the involvement of (a primarily motoric) thalamic structure for biological motion perception is exciting, as it reveals the need to consider the possibility of a much earlier (pre-cortical) encoding of this special class of motion. As noted, the involvement of earlier-to-develop, deeper structures of the brain for biological motion perception appears to fit well with the extensive behavioral and EEG studies showing that sensitivity to biological motion emerges at birth, or at least early in development (Fox and McDaniel, 1982; Bertenthal, 1996; Hirai and Hiraki, 2005; Méary et al., 2007; Reid et al., 2008). Infants as young as 5 months of age prefer to look at upright walkers over inverted walkers (Fox and McDaniel, 1982), and can discriminate an intact walker from one where the dots have been spatially scrambled (Bertenthal et al., 1987). More recently, it has been shown that the capacity for perceiving biological motion is present at birth. Newborns (two-day-olds) prefer to look at an upright point-light stimulus as compared to its upside-down counterpart, or random motion (Simion et al., 2008). These findings, together with the observed predisposition in newly hatched chicks for looking towards biological motion (Vallortigara et al., 2005; Vallortigara and Regolin, 2006) challenges not only our understanding of the bird's brain but also points to the need to consider earlier, pre-cortical regions in evaluations of the underlying mechanisms for perceiving biological patterns. Of course it is feasible that the representations we observed here in VLN arise later in processing, via descending cortico-thalamic input. Nonetheless our finding of the relevance of a motoric thalamic nucleus, while unexpected and undoubtedly requires further validation with more detailed investigation, appears to fit with existing literature that has implicated the cerebellum in the processing of biological motion (Sokolov et al., 2012), and more broadly, the human thalamus for higher-order behavioral functions (e.g., Bradfield et al., 2013; Habib et al., 2013; Klostermann, 2013; for a review, see Saalmann and Kastner, 2011). Our findings of the involvement of a motor-related subcortical structure for biological motion perception also fit well with the growing body of literature that seems to implicate the mirror neuron system for the perception of socially-relevant stimuli (Tai et al., 2004; Iacoboni and Dapretto, 2006; see also Miller and Saygin, 2013). At the heart of the findings from the social cognition literature is the premise that the perception of biological actions are mapped into the observers' own motor representations (Jeannerod, 2001).

In order to appreciate the functional significance of VLN for biological motion perception, it is important to place our subcortical findings back in the context of responses observed in cortex. The results from our multivariate analyses indicated that both global structure information (global structure vs. local natural), and kinematic information (local natural vs. modified) can be well discriminated in retinotopic regions and extrastriate regions, EBA, FBA, STS and IFG. While the sensitivity of these extrastriate regions is not surprising as these same regions have been previously implicated in biological motion perception, the high prediction accuracies into the early retinotopic regions are surprising and allude to a possible role of low level differences between our stimulus classes which may have been a necessary byproduct of our intended manipulations. For example, one distinct difference between the global walker and the two local stimuli is that the global walker had a fixed configuration (that of a typical human body shape) in the visual field, whereas the two local walkers had a more variable spatial extent. However, we note that as our spatial randomizations for the local stimuli were restricted along the horizontal dimension only, and further restricted within a grid specified by the size of the veridical walker, both the density of the stimuli and the overall spatial extent should be preserved on average across trials. In order to further probe the possible role of low level differences in driving the observed SVM prediction accuracies, we conducted an additional MVPA analysis for the global structure versus kinematics discrimination when both stimulus types are presented upside-down (Supplementary Fig. S3). Interestingly, as compared to the accuracies for the upright stimuli (for the same comparison), prediction accuracies for the inverted variants increased substantially in early visual cortical regions (V1-V4). In extrastriate regions including IFG, EBA, FBA, STS, and even the VLN, however, comparable prediction accuracies were observed for the two orientations. At first glance, the substantial increase in accuracies in early visual cortex for the upsidedown discriminations seems puzzling; however, this increase seems to match the exaggerated difference in behavioral accuracies between the two conditions when the stimuli are turned upside down

(Fig. 2, white versus black bars on the right versus the same bars on the left). That is, inverting the two stimuli results in exaggerated perceptual differences between the two stimuli. Critically, low level differences cannot account for this exaggerated difference as these cues (if any) remain the same regardless of orientation. Thus we may rule out the possibility that the observer (and classifier) relied solely upon irrelevant low-level differences (e.g., spatial extent) to perform the discriminations in early cortical regions (although the same cannot be concluded of extrastriate regions, and VLN). Still, the high prediction accuracies in the extrastriate regions (and VLN) should not be discounted. Indeed, classification performance is well-above chance in these same areas for discriminations between stimuli where low level properties are almost identical (i.e., natural versus modified kinematics) (Fig. 5).

Nonetheless, we fathom that one way to further establish the functional relevance of the high accuracies observed in the early retinotopic regions, as well as extrastriate pSTS, IFG, EBA, and the VLN, is to examine the relationships between these responses and behavior. In Supplementary Fig. S4, we plotted individual subject behavioral performances against SVM accuracies obtained when comparing the local natural and local modified stimuli. This choice was driven by the fact that it provided the highest prediction accuracy in VLN, as compared to other conditions (Fig. 6b) and likely to offer more reliable comparisons. Behavioral performance for these two conditions were first converted into an index, computed as (accuracy_local_modified) subtracted from (accuracy_local_natural). The indices were then plotted against the SVM prediction accuracies for two sample retinotopic regions (V1, V2) as well as for extrastriate pSTS, IFG, EBA, and subcortical VLN. As evident in this figure, behavioral discriminations provide a better match to SVM prediction accuracies in extrastriate pSTS, IFG, EBA, as well as VLN (Figs. S4c, d, e, f) as compared to V1 or V2 (Figs. S4a and b). Still, we caution that interpretation of these relationships is not straightforward, as behavioral discriminations are based on left-right direction judgments, while prediction accuracies are based on conditional differences between walker types.

We finally consider the role of inversion in the present data. As noted, we opted to present the three main walker types both upright and upside-down in light of the extensive behavioral literature suggesting orientation effects relating to structure- and kinematics perception are likely attributable to very different sources. Orientation-dependent modulations observed in the fMRI responses, then, could provide further insight into the specificity of the relevant regions. Our behavioral findings are largely consistent with the orientation-specific behavioral responses to both global structure and local kinematic cues in biological motion demonstrated previously (Troje and Westhoff, 2006; Chang and Troje, 2009; Hirai et al., 2011). The global inversion effect is normally attributed to the retrieval of the familiar shape of the walker as conveyed by the display's spatiotemporal organization. The configuration-based inversion effect was not statistically significant here, possibly due to our additional manipulation of the local trajectories (rendered left-right mirror-symmetric), which acted to decrease discrimination accuracies when the stimulus was held upright. Indeed an examination of our obtained accuracies for the global stimulus at the upright orientation (~80%) indicated that they are significantly lower than those obtained in previous work where local trajectories were held intact along with global shape (~90% in Hirai et al., 2011). The inversion effect for the local natural stimulus, on the other hand, can be attributed to the presence (and orientation) of acceleration (Chang and Troje, 2009). Lastly, what might account for the final inversion effect observed for the local modified stimulus? Due to our manipulation, natural acceleration information is absent in these stimuli. We speculate that here, direction is retrieved by extrinsic motion cues, akin to the translation of a point placed at the rim of rolling wheel (Johansson, 1974). This extrinsic information is reversed when a stimulus is mirror-inverted about the horizontal axis. Indeed, behavioral responses are trending in the opposite direction when the motion is inverted (31% accuracy) rather than upright (66% accuracy) (Fig. 2, grey-fill). We still note that a second cue, notably the vertical layout or location of the individual point-lights, and in particular of the feet, may also underlie the inversion effect for the modified stimulus. Specifically, it has been shown that the magnitude of the local motion-based inversion effect is not only modulated by the orientation of vertical acceleration, but also by whether the vertical order of the body is kept intact (i.e., head at the top, feet at the bottom) (Hirai et al., 2011). In the present study, in order to destroy global structure in our local stimuli, we elected to shuffle the spatial positions of the point-lights about the horizontal axis only, thereby retaining the vertical order of the body. This correspondingly produced a large behavioral inversion effect, as predicted by previous work (Hirai et al., 2011). How did orientation affect fMRI responses?

As evident in Fig. 3, response amplitudes changed very little upon stimulus inversion, across all three types of walkers. Results from the MVPA, however, are again more revealing. Orientation of global form can be well discriminated a number of regions including early visual cortex and the human motion complex (hMT+). By contrast, orientation of local kinematics is not well-discriminated across all ROIs tested (Fig. 5). We can only speculate as to what might account for this apparent discrepancy between the behavioral and fMRI responses. In line with suggestions that the kinematics-based mechanism should be a fast-acting one (Hirai et al., 2011), perhaps responses that reflect local-orientation-sensitivity are temporally transient such that they could not be captured and contrasted well by the long TR of fMRI acquisition. Another potential factor that may contribute to our inability to measure kinematics-based orientation effects under the current paradigm may relate to the traditional fMRI setup in which the observer is laying supine and viewing a mirror tilted above the head. Given previous behavioral data implicating vestibular input for perceiving biological kinematics (Chang et al., 2010), we may have expected to observe orientation-dependent responses in vestibular cortex. Indeed, one previous neuroimaging study has demonstrated the involvement of vestibular cortex when perceiving gravity-consistent visual stimuli (specifically, object motion consistent with natural gravitational acceleration; Indovina et al., 2005). Here, the offset of the stimulus with respect to the gravity vector may have acted to weaken the relevant orientation-dependent responses.

Previous theoretical models (Giese and Poggio, 2003) have posited that biological motion perception occurs in the lateral-occipitotemporal cortex as an end-product of initially segregated cortical streams for basic form (ventral) and kinematic (dorsal) representations. While one previous study has shown involvement of non-cortical (cerebellar) regions for biological motion perception (Sokolov et al., 2012), it unclear as to whether there may be more extensive subcortical involvement that may have been missed in traditional univariate approaches. Here, we introduced subtle manipulations in our stimuli in an attempt to isolate specific aspects of biological motion perception, using a multivariate approach to survey of the networks engaged in biological motion perception. Our data implicate a wide and complex network with extensive cortical sensitivity to biological motion along much of the same areas previously identified by others, but also a surprising capacity of thalamic VLN to make similar discriminations of biological patterns. Although we caution the exact role of this motoric thalamic nucleus in governing sensitivity to biological motion requires careful validation, our finding fits well with previous reports of the involvement of other aspects of the motor loop (Cerebellum; Sokolov et al., 2012). While it is possible that the VLN response arrives from descending cortico-thalamic input to prepare the organism for a response to a potentially-threatening stimulus, the possibility of this area being a part of a much earlier, potentially pre-cortical system that may signal “life” (Troje and Westhoff, 2006; Johnson, 2006) is exciting and deserves further attention and further research.

Author contributions

DC, HB, and NT contributed to stimulus and design development. DC

and HB performed data collection and analyses. All authors contributed to the preparation of this manuscript.

Competing financial interests

The authors declare no competing financial interests.

Acknowledgments

This research was supported by the Foreign Researcher Invitation Program, National Institute of Information and Communications Technology (NICT), Japan, a JSPS KAKENHI (17H04790) to HB, as well as the Ministry of Internal Affairs, Japan (H29 0155-0149).

Appendix ASupplementary data

Supplementary data related to this article can be found at https://doi.org/10.1016/j.neuroimage.2018.03.013.

References

Ban, H., Preston, T.J., Meeson, A., Welchman, A.E., 2012. The integration of motion and disparity cues to depth in dorsal visual cortex. Nat. Neurosci. 15, 636–643.
Baxter, M.G., 2013. Mediodorsal thalamus and cognition in non-human primates. Front. Syst. Neurosci. 7, 38.
Bradfield, L.A., Hart, G., Balleine, B.W., 2013. The role of the anterior, mediodorsal, and parafascicular thalamus in instrumental conditioning. Front. Syst. Neurosci. 7, 51.
Beintema, J.A., Lappe, M., 2002. Perception of biological motion without local image motion. Proc. Natl. Acad. Sci. U. S. A. 99, 5661–5663.
Bertenthal, B.I., Proffitt, D.R., Kramer, S.J., 1987. Perception of biomechanical motions by infants: implementation of various processing constraints. J Exp. Psychol. Hum. Percept. Perform. 13, 577–585.
Bertenthal, B.I., 1996. Origins and early development of perception, action, and representation. Annu. Rev. Psychol. 47, 431–459.
Bonda, E., Petrides, M., Ostry, D., Evans, A., 1996. Specific involvement of human parietal systems and the amygdala in the perception of biological motion. J. Neurosci. 16, 3737–3744.
Bonda, E., Petrides, M., Frey, S., Evans, A., 1995. Neural correlates of mental transformations of the body-in-space. Proc. Natl. Acad. Sci. 92 (24), 11180–11184.
Carpenter, M.B., Strominger, N.L., 1967. Efferent fibers of the subthalamic nucleus in the monkey. A comparison of the efferent projections of the subthalamic nucleus, substantia nigra and globus pallidus. Am. J. Anat. 121, 41–72.
Casile, A., Giese, M.A., 2005. Critical features for the recognition of biological motion. J. Vis. 5 (4), 6–6.
Chang, C.-C., Lin, C.-J., 2011. LIBSVM : a library for support vector machines. ACM Trans. Intel. Syst. Technol. 2 (27), 1–27.
Chang, D.H., Troje, N.F., 2009. Acceleration carries the local inversion effect in biological motion perception. J. Vis. 9 (1), 1–17, 19.
Chang, D.H., Harris, L.R., Troje, N.F., 2010. Frames of reference for biological motion and face perception. J. Vis. 10 (6), 22.
Chawla, N.V., Bowyer, K.W., Hall, L.O., Kegelmeyer, W.P., 2002. SMOTE: synthetic minority over-sampling technique. J. Artif. Intell. Res. 16, 341–378.
Creem-Regehr, S.H., Neil, J.A., Yeh, H.J., 2007. Neural correlates of two imagined egocentric transformations. Neuroimage 35 (2), 916–927.
Daskalakis, Z.J., et al., 2004. Exploring the connectivity between the cerebellum and motor cortex in humans. J. Physiol. 557.2, 689–700.
De Martino, F., et al., 2008. Combining multivariate voxel selection and support vector machines for mapping and classification of fMRI spatial patterns. Neuroimage 43, 44–48.
Dupont, P., De Bruyn, B., Vandenberghe, R., Rosier, A.M., Michiels, J., Marchal, G., Orban, G.A., 1997. The kinetic occipital region in human visual cortex. Cerebr. Cortex (New York, NY: 1991) 7 (3), 283–292.
Fox, R., McDaniel, C., 1982. The perception of biological motion by human infants. Science 218, 486–487.
Freire, A., Lee, K., Symons, L.A., 2000. The face-inversion effect as a deficit in the encoding of configural information: direct evidence. Perception 29 (2), 159–170.
Giese, M.A., Poggio, T., 2003. Neural mechanisms for the recognition of biological motion. Nat. Rev. Neurosci. 4, 179–192.
Gilaie-Dotan, S., Saygin, A.P., Lorenzi, L.J., Rees, G., Behrmann, M., 2015. Ventral aspect of the visual form pathway is not critical for the perception of biological motion. Proc. Natl. Acad. Sci. 112 (4), E361–E370.
Grossman, E.D., Blake, R., 2002. Brain areas active during visual perception of biological motion. Neuron 35, 1167–1175.
Grosbas, M.-H., Beaton, S., Eickhoff, S.B., 2012. Brain regions involved in human movement perception: a quantitative voxel-based meta-analysis. Hum. Brain Mapp. 33, 431–454.
Habib, M.R., Ganea, D., Katz, I.K., Lamprecht, R., 2013. ABL1 in thalamus is associated with safety but not fear learning. Front. Syst. Neurosci. 7, 5.
Hirai, M., Hiraki, K., 2005. An event-related potentials study of biological motion perception in human infants. Cognit. Brain Res. 22, 301–304.
Hirai, M., Chang, D.H., Saunders, D.R., Troje, N.F., 2011. Body configuration modulates the usage of local cues to direction in biological-motion perception. Psychol. Sci. 12, 1543–1549.
Hirai, M., Saunders, D.R., Troje, N.F., 2011. Allocation of attention to biological motion: local motion dominates global shape. J. Vis. 11 (3), 4.
Huk, A.C., Dougherty, R.F., Heeger, D.J., 2002. Retinotopy and functional subdivision of human areas MT and MST. J. Neurosci. 22 (16), 7195–7205.
Iacoboni, M., Dapretto, M., 2006. The mirror neuron system and the consequences of its dysfunction. Nat. Rev. Neurosci. 7 (12), 942–951.
Ide, J.S., Chiang-shan, R.L., 2011. A cerebellar thalamic cortical circuit for error-related cognitive control. Neuroimage 54 (1), 455–464.
Indovina, I., Maffei, V., Bosco, G., Zago, M., Macaluso, E., Lacquaniti, F., 2005. Representation of visual gravitational motion in the human vestibular cortex. Science 308 (5720), 416–419.
Jankowski, M.M., Ronnqvist, K.C., Tsanov, M., Vann, S.D., Wright, N.F., Erichsen, J.T., et al., 2013. The anterior thalamus provides a subcortical circuit supporting memory and spatial navigation. Front. Syst. Neurosci. 7.
Jastoff, J., Orban, G.A., 2009. Human functional magnetic resonance imaging reveals separation and integration of shape and motion cues in biological motion processing. J. Neurosci. 29, 7315–7329.
Johansson, G., 1973. Visual perception of biological motion and a model for its analysis. Percept. Psychophys. 14, 195–204.
Jeannerod, M., 2001. Neural simulation of action: a unifying mechanism for motor cognition. Neuroimage 14 (1), S103–S109.
Johansson, G., 1974. Vector analysis in visual perception of rolling motion. Psychol. Res. 36, 311–319.
Johnson, M.D., Ojemann, G.A., 2000. The role of the human thalamus in language and memory: evidence from electrophysiological studies. Brain Cognit. 42 (2), 218–230.
Johnson, M.H., 2006. Biological motion: a perceptual life detector? Curr. Biol. 16, R376–R377.
Kievit, J., Kuypers, H.G.J.M., 1975. Subcortical afferents to the frontal lobe in the rhesus monkey studied by means of retrograde horseradish peroxidase transport. Brain Res. 85, 261–266.
Kievit, J., Kuypers, H.G.J.M., 1977. Organization of the thalamo-cortical connexions to the frontal lobe in the rhesus monkey. Exp. Brain Res. 29 (3–4), 299–322.
Klostermann, F., 2013. Functional roles of the thalamus for language capacities. Front. Syst. Neurosci. 7, 32.
McAlonan, K., Cavanaugh, J., Wurtz, R.H., 2008. Guarding the gateway to cortex with attention in visual thalamus. Nature 456 (7220), 391.
Méary, D., Kitromilides, E., Mazens, K., Graff, C., Gentaz, E., 2007. Four-day-old human neonates look longer at non-biological motions of a single point-of-light. PloS ONE 2: e186.Peuskens H, Vanrie J, Verfaillie K, Orban GA (2005) Specificity of regions processing biological motion. Eur. J. Neurosci. 21, 2864–2875.
Miller, L.E., Saygin, A.P., 2013. Individual differences in the perception of biological motion: links to social cognition and motor imagery. Cognition 128 (2), 140–148.
Morel, A., Liu, J., Wannier, T., Jeanmonod, D., Rouiller, E.M., 2005. Divergence and convergence of thalamocortical projections to premotor and supplementary motor cortex: a multiple tracing study in the macaque monkey. Eur. J. Neurosci. 21 (4), 1007–1029.
O'Connor, D.H., Fukui, M.M., Pinsk, M.A., Kastner, S., 2002. Attention modulates responses in the human lateral geniculate nucleus. Nat. Neurosci. 5 (11), 1203.
O'toole, A.J., Natu, V., An, X., Rice, A., Ryland, J., Phillips, P.J., 2014. The neural representation of faces and bodies in motion and at rest. NeuroImage 91, 1–11.
Ostendorf, F., Liebermann, D., Ploner, C.J., 2013. A role of the human thalamus in predicting the perceptual consequences of eye movements. Front. Syst. Neurosci. 7, 10.
Peelen, M.V., Wiggett, A.J., Downing, P.E., 2006. Patterns of fMRI activity dissociate overlapping functional brain areas that respond to biological motion. Neuron 49 (6), 815–822.
Peuskens, H., Vanrie, J., Verfaillie, K., Orban, G.A., 2005. Specificity of regions processing biological motion. Eur. J. Neurosci. 21 (10), 2864–2875.
Prevosto, V., Graf, W., Ugolini, G., 2009. Cerebellar inputs to intraparietal cortex areas LIP and MIP: functional frameworks for adaptive control of eye movements, reaching, and arm/eye/head movement coordination. Cereb. cortex 20 (1), 214–228.
Prevosto, V., Sommer, M., 2013. Cognitive control of movement via the cerebellar-recipient thalamus. Front. Syst. Neurosci. 7, 56.
Ramnani, N., 2012. Frontal lobe and posterior parietal contributions to the cortico-cerebellar system. Cerebellum 11 (2), 366–383.
Reid, V.M., Hoehl, S., Landt, J., Striano, T., 2008. Human infants dissociate structural and dynamic information in biological motion: evidence from neural systems. Soc. Cognit. Affect. Neurosci. 3, 161–167.
Saalmann, Y.B., Kastner, S., 2011. Cognitive and perceptual functions of the visual thalamus. Neuron 71 (2), 209–223.
Saygin, A.P., Wilson, S.M., Hagler, D.J., Bates, E., Sereno, M.I., 2004. Point-light biological motion perception activates human premotor cortex. J. Neurosci. 24 (27), 6181–6188.
Saygin, A.P., 2007. Superior temporal and premotor brain areas necessary for biological motion perception. Brain 130 (9), 2452–2461.
Serences, J.T., 2004. A comparison of methods for characterizing the event-related BOLDtimeseries in rapid fMRI. NeuroImage 21, 1690–1700.
Sereno, M.I., et al., 1995. Borders of multiple visual areas in humans revealed by functional magnetic resonance imaging. Science 268, 889–893.
Shinoda, Y., Kakei, S., Futami, T., Wannier, T., 1993. Thalamocortical organization in the cerebello-thalamo-cortical system. Cereb. Cortex 3, 421–429.
Simion, F., Regolin, L., Bulf, H., 2008. A predisposition for biological motion in the newborn baby. PNAS 150, 809–813.

Sokolov, A.A., et al., 2012. Biological motion processing: the left cerebellum communicates with the right superior temporal sulcus. Neuroimage 59, 2824–2830.
Sunaert, S., Van Hecke, P., Marchal, G., Orban, G.A., 1999. Motion-responsive regions of the human brain. Exp. Brain Res. 127 (4), 355–370.
Tai, Y.F., Scherfler, C., Brooks, D.J., Sawamoto, N., Castiello, U., 2004. The human premotor cortex is' mirror' only for biological actions. Curr. Biol. 14 (2), 117–120.
Talairach, et al., 1988. Co-planar Stereotaxic Atlas of the Human Brain. Thieme, New York.
Thompson, J.C., Baccus, W., 2012. Form and motion make independent contributions to the response to biological motion in occipitotemporal cortex. Neuroimage 59, 625–634.
Thompson, J.C., Clarke, M., Stewart, T., Puce, A., 2005. Configural processing of biological motion in human superior temporal sulcus. J. Neurosci. 25 (39), 9059–9066.
Tomasi, D., Chang, L., Caparelli, E.C., Ernst, T., 2007. Different activation patterns for working memory load and visual attention load. Brain Res. 1132, 158–165.
Troje, N.F., 2002. Decomposing biological motion: a framework for analysis and synthesis of human gait patterns. J. Vis. 2, 371–387.
Troje, N.F., Westhoff, C., 2006. The inversion effect in biological motion perception: evidence for a “life detector”? Curr. Biol. 16, 821–824.
Vallortigara, G., Regolin, L., Marconato, F., 2005. Visually inexperienced chicks exhibit spontaneous preference for biological motion patterns. PLoS Biol. 3, e208.
Vallortigara, G., Regolin, L., 2006. Gravity bias in the interpretation of biological motion by inexperienced chicks. Curr. Biol. 16, R279–R280.
van der Salm, S.M., van der Meer, J.N., Nederveen, A.J., Veltman, D.J., van Rootselaar, A.F., Tijssen, M.A., 2013. Functional MRI study of response inhibition in myoclonus dystonia. Exp. Neurol. 247, 623–629.
van Kemenade, B.M., Muggleton, N., Walsh, V., Saygin, A.P., 2012. Effects of TMS over premotor and superior temporal cortices on biological motion perception. J. Cognit. Neurosci. 24 (4), 896–904.
Vangeneugden, J., Peelen, M.V., Tadin, D., Battelli, L., 2014. Distinct neural mechanisms for body form and body motion discriminations. J. Neurosci. 34 (2), 574–585.
Wandell, B.A., Brewer, A.A., Dougherty, R.F., 2005. Visual field map clusters in human cortex. Philos. Trans. R. Soc. Lond. B Biol. Sci. 360 (1456), 693–707.
Wang, Y., Brzozowska-Prechtl, A., Karten, H.J., 2010. Laminar and columnar auditory cortex in avian brain. Proc. Natl. Acad. Sci. U. S. A. 107 (28), 12676–12681.
Wiesendanger, R., Wiesendanger, M., 1985a. The thalamic connections with medial area 6 (supplementary motor cortex) in the monkey (Macaca fascicularis). Exp. Brain Res. 59 (1), 91–104.
Wiesendanger, R., Wiesendanger, M., 1985b. Cerebello-cortical linkage in the monkey as revealed by transcellular labeling with the lectin wheat germ agglutinin conjugated to the marker horseradish peroxidase. Exp. Brain Res. 59 (1), 105–117.
Xiang, H., Lin, C., Ma, X., Zhang, Z., Bower, J.M., Weng, X., Gao, J.H., 2003. Involvement of the cerebellum in semantic discrimination: an fMRI study. Hum. Brain Mapp. 18 (3), 208–214.